Molecular Crystals and Liquid Crystals Science and Technology. Section A. Molecular Crystals and Liquid Crystals

Publication details, including instructions for authors and subscription information:
http://www.tandfonline.com/loi/gmcl19

DFT Description of Mixed Valence Magnetic Systems. Mn(III)-Mn(IV) and Fe(II)-Fe(III) Complexes

Alessandro Bencini [a] , Dante Gatteschi [a] , Maurizio Mattesini [a] , Federico Totti [a] & Ilaria Ciofini [b]

[a] Dipartimento di Chimica, Università di Firenze, Via Maragliano 75, 50144, Firenze, Italia

[b] Institut de Chimie Inorganique et Analytique, Université de Fribourg, Pérolles, 1700, Fribourg, Switzerland

Version of record first published: 24 Sep 2006

Mol. Cryst. and Liq. Cryst., 1999, Vol. 335, pp. 665-674
Reprints available directly from the publisher
Photocopying permitted by license only

DFT Description of Mixed Valence Magnetic Systems. Mn(III)-Mn(IV) and Fe(II)-Fe(III) Complexes

ALESSANDRO BENCINI[a], DANTE GATTESCHI[a], MAURIZIO MATTESINI[a], FEDERICO TOTTI[a] and ILARIA CIOFINI[b]

[a]*Dipartimento di Chimica, Università di Firenze, Via Maragliano 75, 50144, Firenze, Italia and* [b]*Institut de Chimie Inorganique et Analytique, Université de Fribourg, Pérolles, 1700 Fribourg, Switzerland*

Density functional theory has been successfully applied to characterize the electronic structure and the magnetic properties of the mixed-valence dinuclear complex $[Fe_2(OH)_3(tmtacn)_2]^{2+}$[1],[2], modeled by replacing the tmtacn ligand with 3 ammonia molecules, and the complex $[Mn_2(O)_2(NH_3)_8]^{3+}$[3], where the ammonia modeled two Tren ligands. Spectroscopic and magnetic properties have been computed in nice agreement with the experimental values. Minimum energy path calculations allowed us to compute the frequencies ν_- associated to the normal coordinate Q_- responsible of the delocalization of the extra electron and we present here a procedure for the full characterization of mixed-valence transition metal dimers.

Keywords: Mixed Valence; Iron; Manganese; Double Exchange; Potential Surfaces; Broken Symmetry

INTRODUCTION

The modeling of valence trapping phenomena, which is required in order to have a deeper insight into the electronic structure of mixed valence compounds, requires the knowledge of the potential energy surface of the system as a function of the position of the atomic nuclei. Since rather small geometrical variations (~ 0.1 Å in bond distances and ~ 1° in bond angles) can be indicative of valence trapping, a method of calculation is needed which can reproduce the energy changes upon small nuclear displacements with sufficient accuracy and which can be applied to large molecular systems containing transition metal ions. The Density Functional Theory[4] combined with the Broken Symmetry approach[5] has been resulted well suited to

reproduce the electronic structure of mixed valence systems including the calculation of adiabatic potential surfaces. The iron complex is an example of complete delocalized mixed valence system and has already been studied[6]. Here we review the results for the iron compound and report the preliminary results of the model applied to Mn(III)-Mn(IV) compound as an example of of localized mixed valence system[7]. These systems have great relevance in both biological, as models for catalytic center for the oxidation of water to molecular oxygen of photosystem II[8], and solid state chemistry (e.g. $Ln_{1-x}A_xMnO_3$ [Ln = rare-earh, A = divalent cation] compounds which shows the Colossal Magneto-Resistance phenomenon)[9],[10].

Computational Details

Iron compound

Electronic calculations were performed with the Amsterdam Density Functional (ADF) program package, version 2.2.[11] The standard basis sets provided within the package were used throughout. Double-ζ STO basis sets were applied to the valence electrons of all non hydrogen atoms, except the iron *3d* orbitals which were represented using a triple-ζ function. The shells up to *3p* for Fe and *1s* for all the other non hydrogen atoms were treated as frozen cores. Single-ζ STO basis sets were used for hydrogen atoms.

To compute the spectromagnetic properties of $[Fe_2(OH)_3(tmtacn)_2]^{2+}$, we have modeled it by replacing the tmtacn ligand (= N,N',N"-trimethyl-1,4,7-triazacyclononane) by 3 ammonia molecules.

In preliminary calculations various approximations to the exchange correlation potential were used. The VWN-Stoll approximation to the exchange-correlation potential includes the local potential of Vosko, Wilk and Nusair[12] with added the Stoll's correlation[13] correction term. Gradient corrections to the exchange and correlation potentials were applied in the form proposed by Becke[14] for the exchange part and by Perdew[15] for the correlation, or using the more recent Perdew and Wang[16],[17] exchange-correlation corrections. The VWN-Stoll approximation was used in all the other calculations.

Anharmonic frequencies needed for the estimation of vibronic couplings (*vide infra*) were computed with the DiNa package[18].

Manganese compound

Double-ζ STO basis sets were applied to the valence electrons of all non-hydrogen atoms with the exception of the *3d* orbitals of the Mn which are reproduced by triple-ζ STO basis functions. The shells up to the *2p* for Mn

and the *1s* for all the other non hydrogen atoms have been treated as frozen cores. Single-ζ STO basis sets have been used for hydrogen atoms. The VWN-Stoll approximation to the exchange-correlation potential which includes the local potential of Vosko, Wilk, and Nusair with added the Stoll's correlation correction term has been applied in all calculations.

The experimental structure of the di-nuclear MV manganese complex have modeled by substituting the aliphatic amine capping ligands (tren) with eight ammonia molecules.

The linear transit approach has been used to investigate the nuclear potential surface with respect to the antisymmetric displacement, Q_-, of the plane individuated by the plane passing the two oxygens and orthogonal to the direction individuated by the two manganese atoms.

Results and Discussion

Iron.

Spectro-magnetic properties. The model molecule, and the relevant geometrical parameters used in the calculations are shown in Fig. 1.

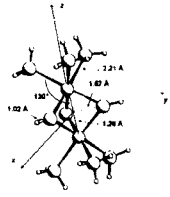

FIGURE 1 Model geometry

The geometries optimized with the above constraints on the high spin S=9/2 state using different functionals show that the inclusion of non local corrections leads to larger Fe-Fe distances as compared to the experimental values. Since the best agreement were computed with the VWN-Stoll functional[12],[13], all the following results were obtained using with this functional. More details are given in ref. [6]. The structure obtained by the full geometry optimization also agrees rather well with the experimental findings, except for a distortion of the Fe-Fe-N angle to a lower value which is probably not allowed by the macrocyclic ligand.

The one-electron energy levels computed for $[Fe_2(OH)_3(NH_3)_6]^{2+}$ in the high spin state S=9/2 are shown in Fig. 2. The 11 α spin electrons are occupying orbitals which are mainly composed by *3d* iron orbitals, except the orbital $2a_2'$ which is a linear combination of in-plane *2p* orbitals of the oxygen atoms. The highest occupied β orbitals correspond to the $2a_2'$ and $6a_1'$, yielding a total of 9 unpaired electrons. The $6a_1'$ orbital is the in-phase linear combination of the z^2 orbitals of both Fe centers and, this strongly metal-metal bonding orbital is almost completely localized onto the two

metals with a small contribution from in-plane *2p* orbitals of the oxygens. The antibonding counterpart is $5a_2''$ and it is singly occupied. In this molecular orbital the z^2 orbitals can interact with the $2p_z$ oxygen orbitals, which are perpendicular to the O_3 plane, and the computed gross atomic orbital population is consequently smaller (69% *vs.* 94%). The *e* type orbitals are rather strongly interacting with the oxygen orbitals and are responsible for the super-exchange contributions to the magnetic interaction between the metals.

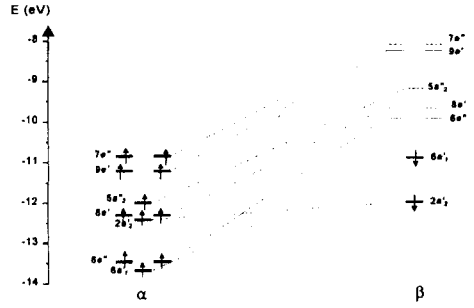

FIGURE 2 Electronic Structure of $[Fe_2(OH)_3(NH_3)_6]^{2+}$

Two high spin S=9/2 states can arise according to the double occupation of the $6a_1'$ or $5a_2''$ orbitals, respectively, whose energy difference is in the spin hamiltonian approach 10B[19]. The electronic transitions were computed using the Slater transition state formalism[20] in C_{2v} symmetry (with the C_2 axis perpendicular to the Fe-Fe bond) in order to distinguish between the orbitals belonging to degenerate (*e*) representations of the D_{3h} point group. The transition energies are in general agreement with the experimental ones and with those previously obtained by Xα-SW calculations[1],[2]. The computed energy for the transition $6a_1' \rightarrow 5a_2''$, which we can call also $\sigma \rightarrow \sigma^*$, is very close to the experimental value, while all the calculations suggest a reverse ordering for the two high energy bands. From the energy of the transition $6a_1' \rightarrow 5a_2''$ we compute B = 1366 cm^{-1} to be compared with the experimental value of 1350 cm^{-1}.

The calculation of the exchange-coupling constant, J, appearing in equation (1) requires the knowledge of the energy of a spin state with spin multiplicity S different from 9/2. The description of low spin states generally requires the use of state functions which are linear combinations of Slater

determinants and therefore cannot be handled within conventional DFT[4]. We handled this situation by the BS formalism which employs the energy of a reference state of mixed spin and space symmetry, the BS state, obtained by imposing two high spin states on the different iron centers with opposite spins[21]. The key equation which allows the calculation of J is:

$$E_{av}(S_{max}) - E(BS) = 2JS_AS_B \qquad (1)$$

where $E_{av}(S_{max})$ is the average of the energies of the high spin states obtained through the transition $\sigma \rightarrow \sigma^*$ *via* two separate SCF calculations, E(BS) is the energy of the BS state and S_A and S_B are the maximum spins on the two metal centers. In the present case the BS determinant represents a state with M_S=1/2 (M_{S_A} = -2, M_{S_B} = 5/2). Equation (1) gives $E_{av}(\frac{9}{2}) - E(BS) = 10J$ from which we get J =137 cm^{-1}.

The BS orbitals are generally taken as good representations[21],[22],[23] for the *natural magnetic orbitals* in weakly coupled systems and are widely used for a qualitative understanding of the magnetic interactions in terms of their overlap[19].

The BS orbitals are localized onto the two different halves of the molecule depending on the overlap between the orbitals forming the symmetric and anti-symmetric molecular orbitals. Strong overlap causes a small localization and indicates the presence, *e.g.*, of a direct metal-metal interaction. In fact, the *in-phase* combination of the z^2 metal orbitals results not well localized as a consequence of the strong overlap between the atomic orbitals, which is responsible of a net metal-metal bond. A significant overlap occurs between the magnetic orbitals through the oxygen atoms suggesting antiferromagnetic super-exchange pathways which must be more efficient between the 13*e* pair of spin-orbitals.

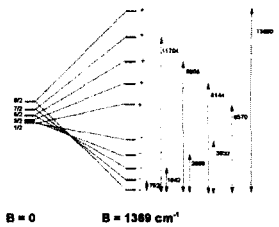

FIGURE 3 Spin multiplets

Using the spin Hamiltonian in [15] and the calculated values of J and B we obtain the relative ordering of the spin multiplets shown in Fig. 3.

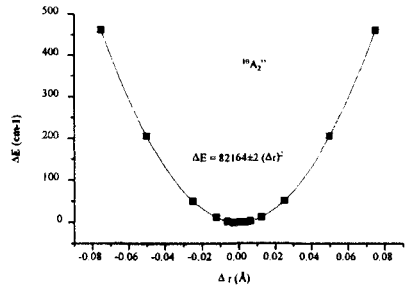

FIGURE 4 Potential Surface of the ground State

On the left hand side the energy level ordering for B = 0 is shown. The low spin state S=1/2 is the ground state as a consequence of the overall antiferromagnetic exchange interaction. The effect of the double-exchange interaction, through the parameter B, is that of stabilizing the high spin state S=9/2. The next spin state, S=7/2, lies 752 cm^{-1} higher in energy, in good agreement with the measured temperature dependence of the magnetic susceptibility which indicates a lower limit of 720 cm^{-1} for the energy separation between the S=7/2 and S=9/2 spin states[1]. It is worth noting that experimental techniques do not allow the separate measure of J and B. It is therefore of importance to have a method of calculation of J which can give an independent estimate of the exchange interaction.

Adiabatic Potential Surfaces: High spin state. The ground state properties of the mixed valence systems depend both from static and dynamic mechanisms which determine the actual values of B and J. The effect of nuclear displacements on the energies of the high spin state has been investigated and a vibronic coupling mechanism in which the out-of-phase combination of the breathing motions on the two monomeric subunits, Q_-, has been claimed to be responsible for electron localization[24]. In the facial bioctahedral dimers this coordinate corresponds to an a_2'' normal mode in D_{3h} symmetry, which becomes a_1 in C3v symmetry. The principal component to this nuclear displacement is the parallel shift of the $(OH)_3$ plane along the C_3 axis concomitant with an out-of phase variation of the metal-nitrogen distances. Since in the complex investigated experimentally the rigid macrocyclic ligands should reduce the importance of these latter displacements (as already observed for the other vibrational modes) we have exploited the potential surface of the system by displacing the $(OH)_3$ plane along the *z* axis keeping the Fe-Fe distance at the value of 2.512 Å and all the other geometrical parameters frozen. The curve computed for the S=9/2 ground state is shown in Fig. 4.

The points on the x axis represent the distance of the $(OH)_3$ plane from the origin, $\Delta r = 0$ corresponding at the symmetric D_{3h} geometry in which the two Fe atoms have equal Fe-O distances. At each point of the curve we did also compute the energy of the σ^* excited state using the Slater transition state procedure[25], which shows a similar harmonic behaviour. The points nicely follow a parabola in the form $y = a + bx^2$ (full line) indicating that the minimum in the energy function corresponds to a completely symmetrical dimer.

Although the previous results well agree with the experimental data, we found of interest to derive from them the parameters widely used to analyze the relative role of vibronic and double-exchange effects. All the analysis has been carried out by the program package DiNa[26]. The results show that the motion is essentially harmonic (the difference between actual frequencies and their harmonic approximation being lower than 5 cm^{-1}). Vibrational frequencies ranging between 360 and 330 cm^{-1} depending on the model used (rigid displacement of the $(OH)_3$ plane or constrained geometry optimization) were computed. The agreement with the experimental estimate[27] of 306 cm^{-1} paves the route to the completely *a priori* determination of all of the parameters (J, B, ν.) entering the phenomenological Hamiltonian describing the electronic structure of mixed-valence dimers. Furthermore, the computed ν. decreases to 210 cm^{-1} for a Fe-Fe distance of 2.75 Å indicating the onset of more important vibronic effects.

Manganese.

Magnetic properties. The geometrical parameters of the modelled system were obtained by geometrical optimization at VWN+Stoll level. The model system is shown in Fig. 5. The computed parameters are in quite good agreement with the experimental ones. (Tab. 1). In fact, the different enviroments relative to the Mn(III) and Mn(IV) have been reproduced, as far as the axial Mn(III)-N distance is more elongated than the equatorial one (Jahn-Teller effect) and the two Mn(IV)-N (axial and eqautorial) distance are almost equivalent, not showing any kind of distortions.

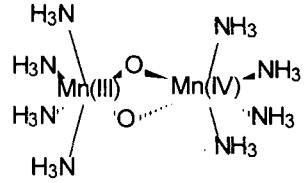

FIGURE 5 The model geometry

Table 1 Relevant geometrical parameters of $[Mn_2(O)_2(NH_3)_8]^{3+}$ obtained by geometry optimization at VWN(Stoll) level:

Geom. Parametrs	Calculated	Experimental
$d_{Mn(III)Mn(IV)}$, Å	2.750	2.679
$d_{Mn(III)O}$, Å	1.907	1.849
$d_{Mn(IV)O}$, Å	1.794	1.774
$d_{Mn(III)N_{ax}}$, Å	2.341	2.260
$d_{Mn(IV)N_{ax}}$, Å	2.032	2.049
$d_{Mn(III)N_{eq}}$, Å	2.117	2.113
$d_{Mn(IV)N_{eq}}$, Å	2.026	2.097

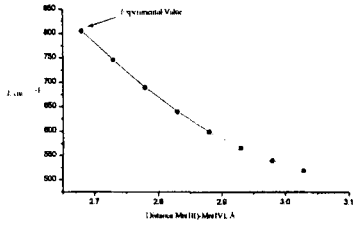

FIGURE 6 The dipendence of J with respect to Mn-Mn distance

The computed J value has been found to be antiferromagnetic and it differs from the experimental value for more than a factor of 2, as usual found out using the BS approach on dinuclaer transition metal compounds[22],[28].

The dependence of J on several structural variations, i.e. Mn-Mn distance and O-Mn-O angle, has been also investigated. While the latter variation has not a great effect on J, the former one almost halves the value from ~800 cm^{-1}

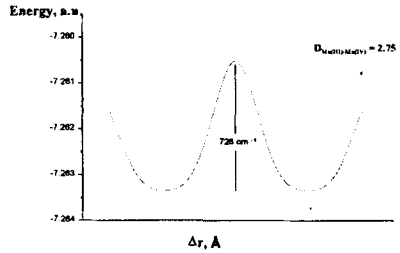

FIGURE 7 Potential Surface of the ground State for d_{Mn-Mn} = 2.75 Å

to ~500 and is shown in Fig. 6.

Adiabatic surfaces. The adiabatic potential energy surface for $[Mn_2(O)_2(NH_3)_8]^{3+}$ complex has been computed by a constrained geometry optimization of the molecule for several values of the Mn-Mn distance and varying the position of the O_2 moiety preserving the orthogonality of O-O and Mn-Mn directions. This procedure is similar to that adopted for the iron complex and assumes that the main contribution to the normal mode responsible for the electron delocalization is the displacement of the O_2 group[29]. The results of the calculations for two Mn-Mn distances are shown in Fig. 7 and 8. The curve in Fig. 7 is an interpolation of the computed points. In both cases the geometry in which the two Mn atoms are in identical environment (Δr = 0 Å) is at higher energy with respect to a distorted situation, which represent a minimum on the potential energy surface. The energy difference this minimum and the energy at Δr = 0 Å is the potential energy barrier for the electron transfer between the two Mn(III)-Mn(IV). Although this barrier lowers with increasing the Mn-Mn distance, this is always computed higher than a vibrational quantum at room temperature, indicating that this complex is to be classified as a Class II (completely localized) mixed valence system[7]. These findings are in agreement with a lot of experimental data on a number of Mn(III)-Mn(IV) doubly oxygen bridged complexes[30].

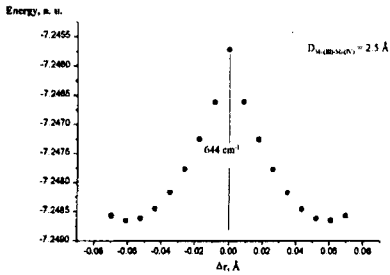

FIGURE 8 Potential Surface of the ground State for d_{Mn-Mn} = 2.50 Å

Conclusions.

We have applied DFT to characterize the electronic structure of two different kind of mixed valence complexes: Fe(II)-Fe(III) and Mn(III)-Mn(IV). The computed potential surfaces clearly show that these two systems belong to Class III and Class II,[7] respectively, in agreement with all the spectroscopic data. DFT is therefore a powerful tool in fully describing the electronic

structure of mixedvalence systems. For the Fe complex, it was also possible to compute the value of the double exchange parameter, B, in close agreement with the experiment. In Class III compound this is related to a metal to metal charge transfer transition. Less accuracy has been obtained in computing the J values in the Mn complex. These were found to be roughly twice as larger than the experimental ones. Since J values are much more sensitive to small geometrical deformations of the environment and to the actual nature of the external ligands than electronic transitions, the choice of the model compound can be responsible for this.[28]

References

[1] D. R. Gamelin, L. Bominaar, M. L. Kirk, K. Wieghardt, E. I. Solomon, *J. Am. Chem. Soc.*, **118,** 8085, (1996).
[2] D. R. Gamelin, L. Bominaar, C. Mathonière, M. L. Kirk, K. Wieghardt, J.-J. Girerd, E. I. Solomon, *Inorg. Chem.*, **35,**4323, (1996).
[3] K. S. Hagen, W. H. Armstrong. H. Hope, *Inorg. Chem.*, **27,** 969,(1988).
[4] R. G. Parr, W. Young, in *Density Functional Theory of Atoms and Molecules,* edited by Oxford University Press (New York, 1989).
[5] L. Noodleman, E. J. Baerends. *E.J. J. Am. Chem. Soc.*, **106,** 2316, 1984.
[6] V. Barone, A. Bencini, I. Ciofini. C. A. Daul, and F. Totti, *J. Am. Chem. S.*, in press.
[7] M. B. Robin, P. Day, *Adv. Inorg. Chem. Chem. Radiochem.*, **10,** 247, (1967).
[8] V. L. Pecoraro, in *Manganese Redox Enzymes*, edited by VCH Publishers (New York, 1992).
[9] G. H. Jonker and J. H. van Santen, *Physica* (Amsterdam), **16,** 337, (1950).
[10] J. H. van Santen and G. H. Jonker, *Physica* (Amsterdam), **16,** 599, (1950).
[11] ADF 2.2, ADF 2.3, Theoretical Chemistry, Vrije Universiteit, Amsterdam.
[12] S. H. Vosko, L. Wilk, M. Nusair. *Canadian J. Phys.*, **58,** 1200, (1980).
[13] H. Stoll, C. M. E. Pavlidou, H. Preuss, *Theor. Chim. Acta*, **49,** 143, (1978).
[14] A. D. Becke, *Phys. Rev. A*, **38,** 3098, (1988).
[15] J. P. Perdew, *Phys. Rev. B*, **33,** 8822, (1986).
[16] J. P. Perdew, Y. Wang, *Phys. Rev. B*, **33,** 8800,(1986).
[17] J. P. Perdew, J. A. Chevary, S. H. Vosko, K. A Jackson; M. R. Pederson, D. J Singh,. *Phys. Rev. A*, **46,** 6671, (1992).
[18] V. Barone, in *Recent Advances in Density Functional Methods;* edited by D. P. Chang, (World Scientific, Singapore, 1996), Vol. 1, p. 287.
[19] O. Kahn, *Molecular Magnetism,* edited by VCH Publishers (New York, 1993).
[20] J. C. Slater, *Quantum Theory of Molecules and Solids* vol. 4; McGraw-Hill; New York; 1974.
[21] L. Noodleman, C. Y. Peng, D. A. Case, J.-M. Mouesca, *Coord. Chem. Rev.*, **144,** 199, (1995).
[22] A. Bencini, F. Totti, C. A. Daul, K. Doclo, P. Fantucci, V. Barone, Inorg. Chem, **36,** 5022, (1997).
[23] A. Bencini, *J. Chim. Phys.* ***86,*** 763, (1989).
[24] G. Blondin, J.-J. Girerd, *Chem. Rev.*, **90,** 1359, (1990).
[25] J. C. Slater, in *Quantum Theory of Molecules and Solids,* edited by McGraw-Hill (New York, 1974).
[26] DiNa Program, Release 2.1, by V. Barone, University of Naples.
[27] D. R. Gamelin, L. Bominaar, C. Mathonière, M. L. Kirk, K. Wieghardt, J.-J. Girerd, E. I. Solomon, *Inorg. Chem.*, **35,**4323, (1996).
[28] C. Adamo, V. Barone, A. Bencini, F. Totti, I. Ciofini, manuscript in preparation.
[29] S. Satpathy, Z. S. Popovic, and F. R. Vukajlovic, *Phys. Rev. Lett.*, **76,**960, (1996).
[30] S. R. Cooper, G. C. Dismukes, M. P. Kein, anf M. Calvin, *J. Am. Chem. Soc.*, **100,** 7248, (1978).